Supplementary information

Carbide-Derived Carbons: WAXS and Raman Spectra for Detailed Structural Analysis

Riinu Härmas [1], Rasmus Palm [1], Heisi Kurig [1], Laura Puusepp [1], Torben Pfaff [2], Tavo Romann [1], Jaan Aruväli [3], Indrek Tallo [1], Thomas Thomberg [1], Alar Jänes [1] and Enn Lust [1,*]

[1] Institute of Chemistry, University of Tartu; chemistry@ut.ee, Ravila 14a, 50411 Tartu, Estonia
[2] Institute of Physical Chemistry, Justus Liebig University, Heinrich-Buff-Ring 17, 35392 Giessen, Germany
[3] Institute of Ecology and Earth Sciences, University of Tartu; geo@ut.ee, Ravila 14a, 50411 Tartu, Estonia
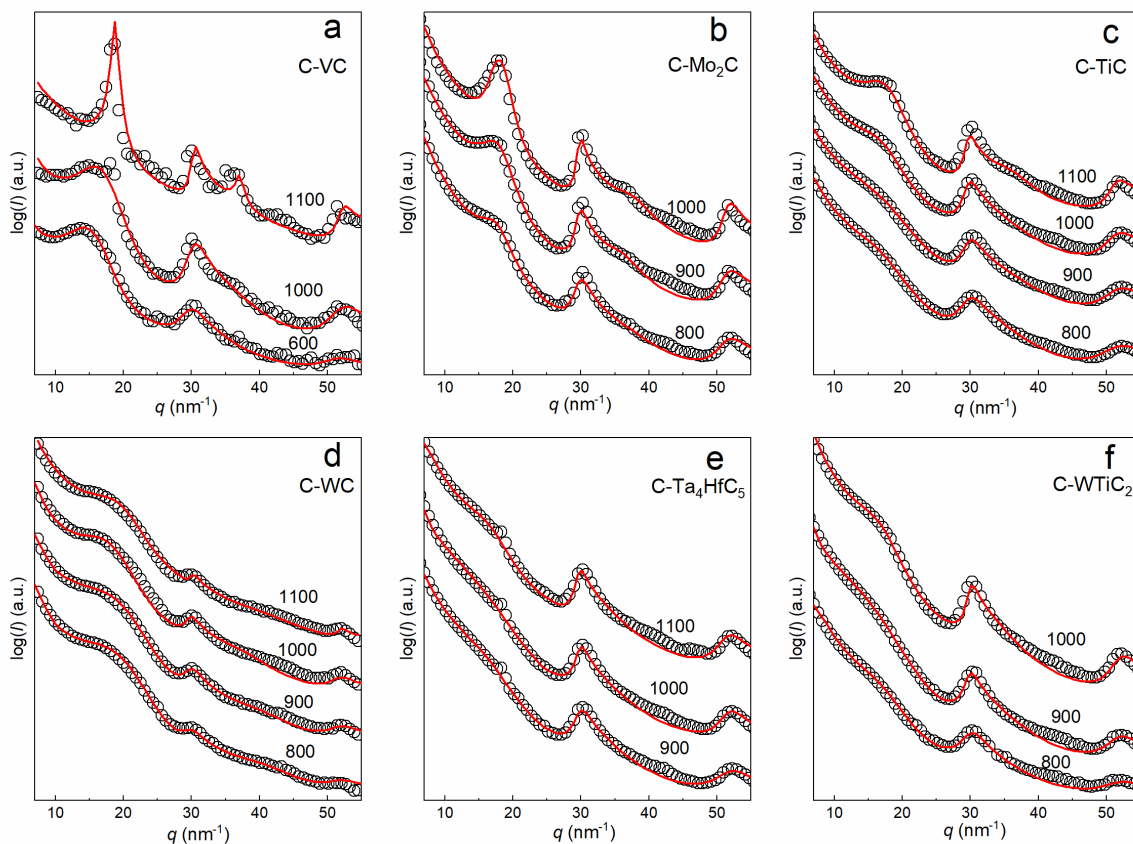[*] Correspondence: enn.lust@ut.ee; Tel.: +372-737-5165

1. WAXS patterns

Figure 1. Wide-angle X-ray scattering data (spheres) of different CDCs (noted in Figure) and fit curve (solid line), of (**a**) C-VC, (**b**) C-Mo2C, (**c**) C-TiC, (**d**) C-WC, (**e**) C-Ta4HfC5 and (f) C-WTiC2 synthesized at different T_{syn} (noted in Fig.). The scattering vector modulus, q, is defined as $q = 4\pi \sin(\theta)/\lambda$, where 2θ is the scattering angle.

Table 1. Parameters derived from WAXS patterns for some CDCs. L_a – average graphene layer extent, $\langle l \rangle$ – average chord length, l_{cc} – average C-C bond length, σ_1 – standard deviation of the first-neighbor

distribution, $\langle N \rangle$ –average number of graphene layers per stack, L_c – average stacking size, κ_c – polydispersity of stack height, a_3 – average interlayer spacing, σ_3 – standard deviation of interlayer spacing.

carbide	T_{syn},°C	L_a, Å	$\langle l \rangle$, Å	l_{cc}, Å	σ_1, Å	$\langle N \rangle$	L_c, Å	κ_c, Å	a_3, Å	σ_3, Å
Error (±%)		10–30	10–15	0.4–1.7	3–21	7–20	5–18	10–15	1–5	20
Mo₂C	800	38	31	1.412	0.16	1.05	12.8	2.4	3.64	0.61
	900	63	50	1.412	0.15	0.79	7.7	1.8	3.54	0.40
	1000	83	67	1.410	0.12	6.74	26.5	0.1	3.51	0.48
TiC	800	26	21	1.410	0.21	1.08	5.0	0.4	3.65	0.38
	900	38	31	1.410	0.19	1.00	4.8	0.3	3.65	0.633
	1000	56	44	1.414	0.18	0.97	5.9	0.7	3.65	0.39
	1100	63	50	1.414	0.14	0.83	8.8	0.5	3.73	0.88
VC	600	25	20	1.42	0.20	1.51	8.2	0.4	3.95	0.51
	1000	29	24	1.41	0.18	1.70	9.8	0.5	3.87	0.73
	1100	63	50	1.406	0.11	0.09	31.4	100.0	3.43	0.11
WC	800	28	22	1.411	0.16	1.40	5.5	0.2	3.14	0.57
	900	33	27	1.409	0.17	1.36	5.3	0.2	3.14	0.48
	1000	45	36	1.411	0.15	1.90	7.5	0.1	3.47	0.21
	1100	50	40	1.421	0.04	1.17	5.6	0.5	3.18	0.02
WTiC₂	800	26	21	1.405	0.22	0.66	3.7	0.6	3.54	0.24
	900	38	31	1.408	0.18	1.36	6.9	0.1	4.53	2.00
	1000	71	57	1.400	0.16	1.02	5.6	0.5	3.69	0.00
Ta₄HfC₅	900	45	36	1.407	0.19	0.86	4.3	0.3	3.76	0.00
	1000	56	44	1.409	0.16	1.21	5.2	0.1	3.80	0.01
	1100	63	50	1.414	0.17	0.53	4.0	1.0	3.75	0.03

Parameter κ_a, polydispersity of chord length, was fixed to 0.25; the lower bound for $a_{3,min}$ was set to 3 Å, since smaller interlayer spacing are physically unlikely. The parameter for thermal motion, u_3, was fixed to 0, as larger values can contribute to the background of the scattering curve. In order to estimate the uncertainties of the calculated parameters, one parameter was changed in CarbX in small steps until the fit quality diminished as seen by emerging fit curve regions exhibiting systematic deviation from the data. In this manner the minimum and maximum values for parameters were obtained and the difference was divided by the average to calculate the percentage.
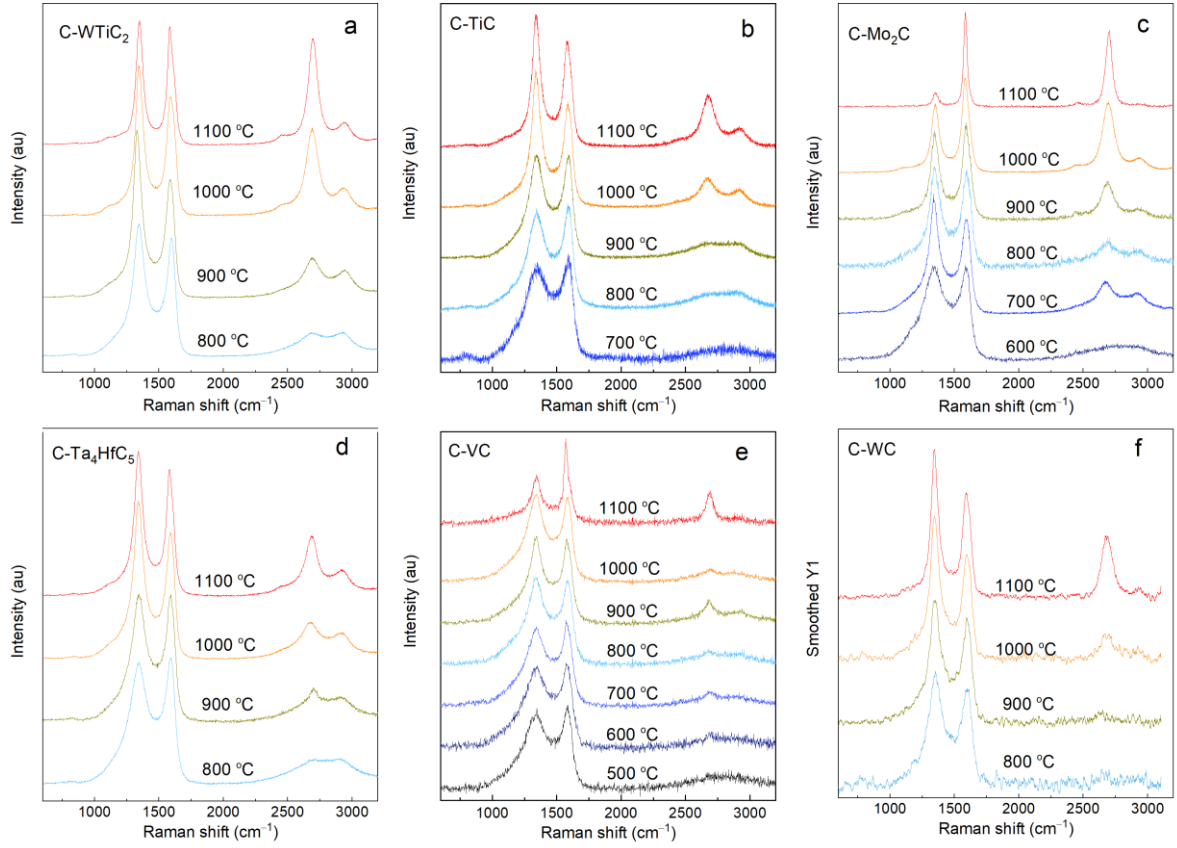
2. Raman spectra

Figure S2. The Raman spectra of (**a**) C-WTiC$_2$, (**b**) C-TiC, (**c**) C-Mo$_2$C, (**d**) C-Ta$_4$HfC$_5$, (**e**) C-VC and (**f**) C-WC synthesized at different T_{syn} (noted in Fig.) and measured with excitation laser wavelength 514 nm (laser energy 2.41 eV).
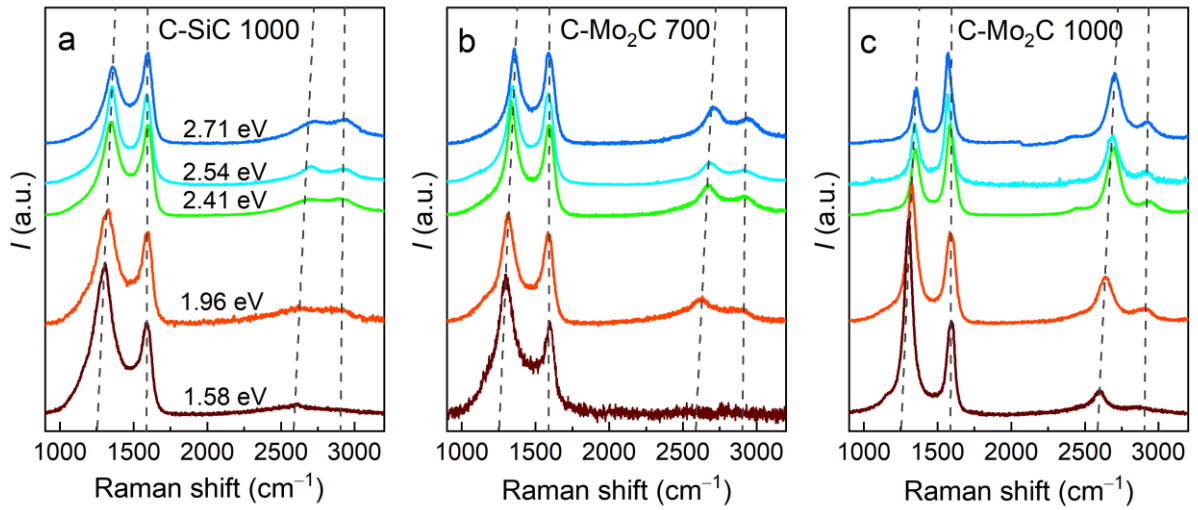
Figure S3. The Raman spectra of (**a**) C-SiC 1000, (**b**) C-Mo$_2$C 700 and (**c**) Mo$_2$C 1000 measured with different laser excitation energies (noted in Fig). The lines connect the band centers, emphasizing the change in the band positions.

2.1 Comparison of different deconvolution approaches

The difference between FWHM obtained with the 3-function (L+L+BWF) deconvolution approach and the 4-or 5-function deconvolution approaches is large for carbons synthesized at lower temperatures $T_{syn} \leq$ 900 °C (i.e for more disordered carbons) but diminishes as the T_{syn} increases (Figure S4a–b). This is to be expected since the intensities of the D$_s$ and G$_s$ bands are also quite low in the Raman spectra of the CDC synthesized at $\geq$ 1000 °C (Figure 3a–c). Thus, the main differences between the 3-function and 4-or 5-function deconvolution approaches are lost.
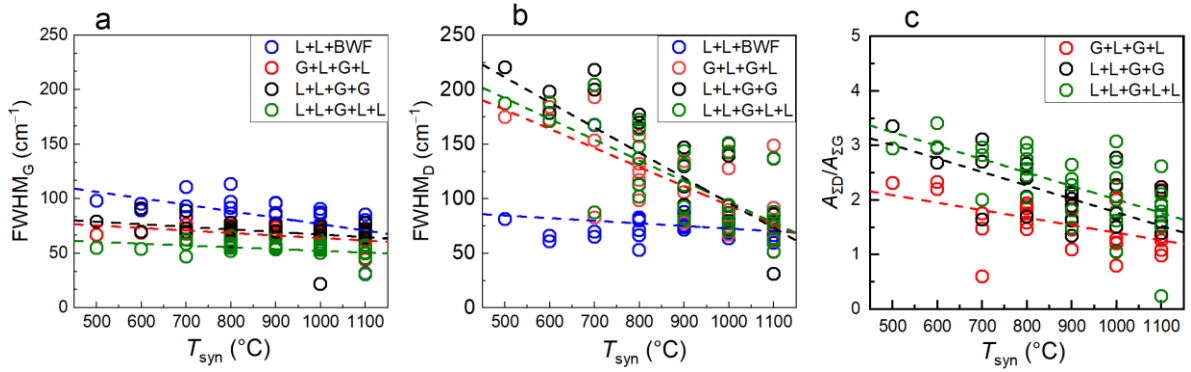

Figure S4. Parameters (a) FWHM$_D$ (b) FWHM$_G$ and (c) $A_{\Sigma D}/A_{\Sigma G}$ (as expressed in Eq. 5). obtained from spectra (E_{laser} = 2.41 eV) of CDCs using different deconvolution methods (noted in Figure) plotted against the synthesis temperature (T_{syn}) of the CDC. The lines given are guides to the eye.

The deconvolution approaches which contained 4 and more distribution functions (G+L+G+L, L+L+G+G and L+L+G+L+L) resulted in a very clear dependence of the FWHM$_D$ on the synthesis temperature (Figure 3f–h, Figure S4c). For the L+L+BWF approach, two Lorentzian shapes were fitted to the experimental D-band, denoted as D$_1$ and D$_2$ (Figure 3a). Neither the FWHM of the D$_1$ nor the FWHM of the D$_2$ demonstrates any dependence on the synthesis temperature of the CDC (Figure 3e, Figure S4c).

The L+L+G+L+L approach was the only approach, which contained the D'-band. The FWHM of the D'-band decreased with T_{syn} for most CDCs (Figure S5).
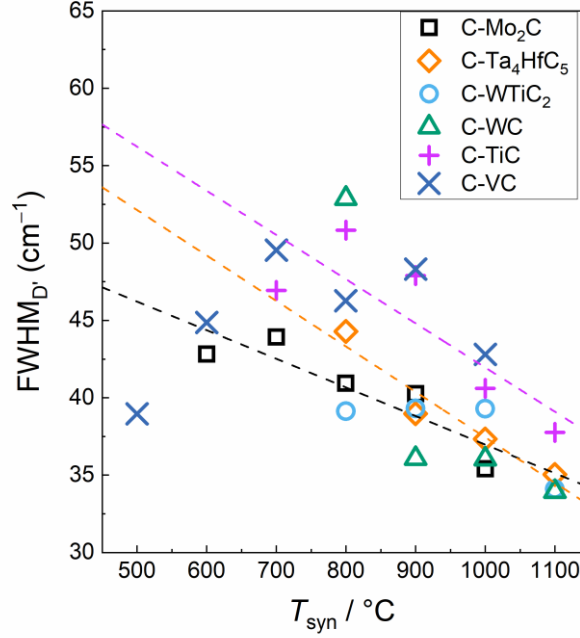
Figure S5. The width of the D'-band (FWHM$_{D'}$) vs the synthesis temperature of the CDC (noted in Figure) obtained with the L+L+G+L+L deconvolution approach.

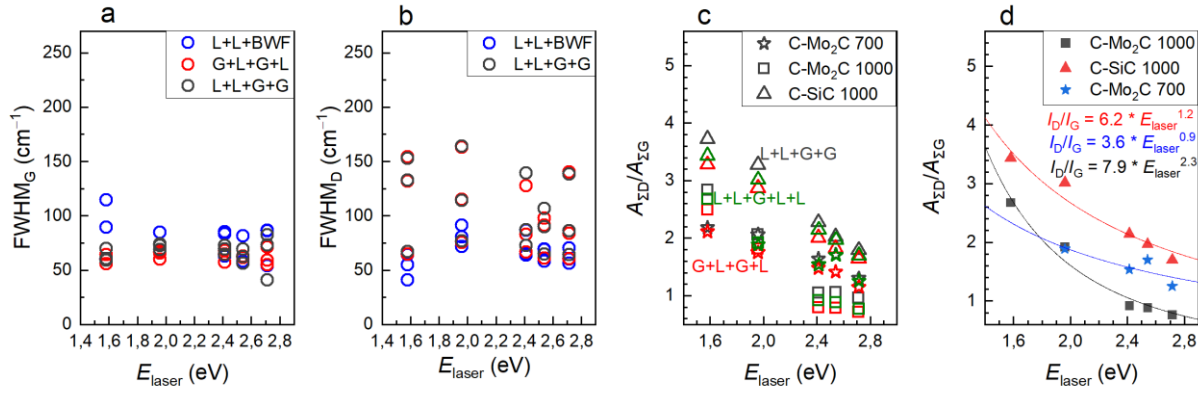*2.1 The impact of different laser excitation energy*

Figure S6. Different parameters obtained from the spectra of C-Mo$_2$C 700, C-Mo$_2$C 1000 and C-SiC 1000 using different deconvolution methods (noted in Figure) plotted against the excitation laser energy (E_{laser}). Full width half maximum of the (**a**) G-band (FWHM$_G$); (**b**) D-band (FWHM$_D$) and (**c**) ratio A$_{ΣD}$/A$_{ΣG}$ (as expressed in Eq. 5). The lines given are guides to the eye. (**d**) The ratio ratio A$_{ΣD}$/A$_{ΣG}$ vs E_{laser}, where the line corresponds to the equation ratio $A_{ΣD}/A_{ΣG}$ = B E_{laser}^x, where parameters B and x are fitted and brought in the graph.
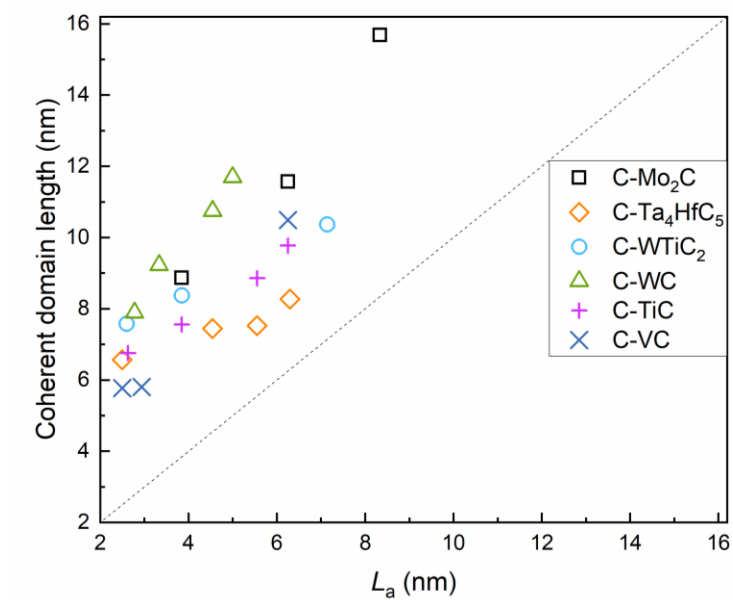
Figure S7. The comparison of the coherent domain length calculated from Raman spectra using ratio $A_{\Sigma D}/A_{\Sigma G}$ and equation $L_a = 490/E_{laser}^4 (A_{\Sigma D}/A_{\Sigma G})^{-1}$ [27] (y-axis) and the graphene domain lengths, L_a, from wide-angle X-ray scattering pattern analysis by CarbX (x-axis).